



# HHS Public Access

Author manuscript

*Biol Psychiatry*. Author manuscript; available in PMC 2016 December 01.

Published in final edited form as:

*Biol Psychiatry*. 2015 December 1; 78(11): 794–804. doi:10.1016/j.biopsych.2015.02.017.

## In Search of Multimodal Neuroimaging Biomarkers of Cognitive Deficits in Schizophrenia

Jing Sui<sup>1,2</sup>, Godfrey D. Pearlson<sup>3,4,5</sup>, Yuhui Du<sup>1,6</sup>, Qingbao Yu<sup>1</sup>, Thomas R. Jones<sup>7</sup>, Jiayu Chen<sup>1</sup>, Tianzi Jiang<sup>2</sup>, Juan Bustillo<sup>7,\*</sup>, and Vince D. Calhoun<sup>1,4,7,8,\*</sup>

<sup>1</sup>The Mind Research Network and Lovelace Biomedical and Environmental Research Institute, Albuquerque, NM, USA, 87106

<sup>2</sup>Brainnetome Center and National Laboratory of Pattern Recognition, Institute of Automation, Chinese Academy of Sciences, Beijing, China, 100190

<sup>3</sup>Olin Neuropsychiatry Research Center, Hartford, CT, USA, 06106

<sup>4</sup>Dept. of Psychiatry, Yale University, New Haven, CT, USA, 06519

<sup>5</sup>Dept. of Neurobiology, Yale University, New Haven, CT, USA, 06519

<sup>6</sup>School of Information and Communication Engineering, North University of China, Taiyuan, China, 030051

<sup>7</sup>Dept. of Psychiatry and Neuroscience, University of New Mexico, Albuquerque, NM, USA, 87131

<sup>8</sup>Dept. of Electronic and Computer Engineering, University of New Mexico, Albuquerque, NM, USA, 87131

### Abstract

**BACKGROUND**—The cognitive deficits of schizophrenia are largely resistant to current treatments, thus are a life-long illness burden. The MATRICS Consensus Cognitive Battery (MCCB) provides a reliable and valid assessment of cognition across major cognitive domains; however, the multimodal brain alterations specifically associated with MCCB in schizophrenia have not been examined.

**METHODS**—The interrelationships between MCCB and the abnormalities seen in three types of neuroimaging-derived maps—fractional amplitude of low frequency fluctuations (fALFF) from resting-state functional magnetic resonance imaging (MRI), grey matter density (GM) from structural MRI and fractional anisotropy (FA) from diffusion MRI, were investigated by using multi-set canonical correlation analysis in data from 47 schizophrenia patients treated with antipsychotic medications and 50 age-matched healthy controls.

---

*Address for Correspondence:* Jing Sui, jsui@mrn.org.

\*Calhoun VD and Bustillo J contributed equally as senior author.

**Publisher's Disclaimer:** This is a PDF file of an unedited manuscript that has been accepted for publication. As a service to our customers we are providing this early version of the manuscript. The manuscript will undergo copyediting, typesetting, and review of the resulting proof before it is published in its final citable form. Please note that during the production process errors may be discovered which could affect the content, and all legal disclaimers that apply to the journal pertain.

The authors report biomedical financial interests or potential conflicts of interest.

**RESULTS**—One multimodal component (CV8) was identified as both group-differentiating and significantly correlated with the MCCB composite. It demonstrated: 1) Increased cognitive performance associated with higher fALFF (intensity of regional spontaneous brain activity) and higher GM volumes in thalamus, striatum, hippocampus, and the mid-occipital region, with co-occurring FA changes in superior longitudinal fascicles, anterior thalamic radiation and forceps major. 2) Higher fALFF but lower GM volume in dorsolateral prefrontal cortex related to worse cognition in schizophrenia. 3) Distinct domains of MCCB might exhibit dissociable multimodal signatures, *e.g.*, increased fALFF in inferior parietal lobule particularly correlated with decreased social cognition. Medication dose did not relate to these findings in schizophrenia.

**CONCLUSIONS**—Our results suggest linked functional and structural deficits in distributed cortico-striato-thalamic circuits may be closely related to MCCB-measured cognitive impairments in schizophrenia.

### Keywords

MATRICES Consensus Cognitive Battery (MCCB); schizophrenia; functional magnetic resonance imaging (fMRI); grey matter; diffusion magnetic resonance imaging (dMRI); multimodal fusion

---

## INTRODUCTION

Interview-based assessments of cognition subsume multiple domains, including attention, working memory, language processing, problem solving, and decision making. Cognitive impairments are recognized as core functional deficits of schizophrenia (SZ), and are a key reason that schizophrenia patients do not successfully re-enter the community (1, 2). Unlike positive symptoms, which may be suppressed by medications, cognitive dysfunction remains in the majority of schizophrenia patients with resulting suboptimal community functioning.

Launched by NIMH, the MATRICS (Measurement and Treatment Research to Improve Cognition in Schizophrenia) Consensus Cognitive Battery (MCCB) is recognized as a valuable tool for comprehensive cognitive function evaluation of schizophrenia in the context of clinical trials. The MCCB includes 10 neurophysiologic tests clustered in 7 cognitive domains (1), including: speed of processing, attention/vigilance, working memory, verbal learning, visual learning, reasoning/problem solving, and social cognition. Despite its widespread use, the neural networks underlying MCCB performance in schizophrenia have been examined in only a few single-modality brain imaging studies (3–5) presenting inconsistent results. Only one study examined MCCB correlates of fused neuroimaging data (MEG and DTI) by joint independent component analysis (6). A posterior visual processing network was related to reduced MEG amplitude, reduced FA and poorer MCCB composite scores in schizophrenia, suggesting the advantage of this fused approach. Currently NIMH emphasizes the importance of “target engagement” in clinical trials (7). Understanding the brain network organization related to MCCB performance may allow imaging assessments to be engaged early in clinical trials; hence accelerates the development of new therapeutic approaches to enhance cognition.

This is the first study to combine functional MRI (fMRI), structural MRI (sMRI) and diffusion MRI (dMRI) with MCCB to generate a full perspective of neuroimaging “targets” of cognitive dysfunction in schizophrenia patients. Nowadays collecting these three types of widely used MRI data from the same subject on one scanner has become a common practice, which can provide comprehensive brain measures of blood flow, gray matter volume and white matter integrity. By taking advantage of the 3-way MRI cross-information and the MCCB in a fusion analysis, we may reveal important covariation that may only partially be detected by a single modality.

## METHODS AND MATERIALS

The study was approved by the Institutional Review Board of University of New Mexico.

### Participants

47 schizophrenia patients and 50 age-matched healthy controls (HC) participated in this study. Demographic data for the subjects are provided in Table 1. Schizophrenia patients were recruited from the University of New Mexico Hospital and the Albuquerque Veterans Administration Medical Center. Healthy controls were recruited from the community through local advertisement. All subjects were screened and excluded if they had diagnosis of central neurological disorder or active substance use disorder (6 month minimum before enrollment, except for nicotine). In addition, healthy controls were excluded if they had first-degree relatives with any psychotic disorder. Patients met criteria for schizophrenia defined by the DSM-IV-TR based on the SCID-P interview (8). All patients were clinically stable on the same antipsychotic medications >4 weeks prior to the scan. Please see Supplementary Table S1 for more information about medication and substance use history. Clinical assessment was performed within 1 week of scanning, using the Positive and Negative Syndrome Scale (PANSS) (9). PANSS raters achieved good inter-rater reliabilities (positive symptom ICC=0.86 and negative symptom ICC=0.64). Informed consent was obtained from all subjects according to institutional guidelines required by the IRB. Subjects were paid for their participation.

### The MCCB

The MCCB (10) was administered within 1 week of imaging. Raw measurement scores were converted to normalized T-scores, resulting in 7 domain T-scores and a composite T-score via the MCCB scoring program. As shown in Table 1, all MCCB scores are significantly lower in SZ and all domain scores are significantly correlated with the composite. No correlation was found between MCCB composite and medication dose in SZ. The domain of speed of processing has the highest correlation ( $R=0.91$ ), consistent with the reports that MCCB composite is usually dominated by the domain of speed of processing (11, 12), which proved to be the best single predictor of overall cognitive performance (13). Additionally, as expected (32, 33), negative PANSS scores had a significant anti-correlation with the MCCB composite ( $R=-0.48$ ,  $p=0.0008$ ).

## Imaging Parameters

All subjects were scanned by fMRI, sMRI and dMRI, which were collected on a 3-Tesla Siemens Trio scanner with a 12-channel radio frequency coil. **fMRI:** Resting-state scans were a minimum of 5 minutes, 4s in duration (152 volumes). Subjects were instructed to keep their eyes open during the scan and stare passively at a presented fixation cross, as this is suggested to facilitate network delineation compared to eyes-closed conditions and helps ensure that subjects are awake. The data were collected with single-shot full k-space echo-planar imaging with ramp sampling correction using the inter commissural line (AC/PC) (anterior commissure/posterior commissure) as a reference (TR=2s, TE=29 ms, matrix size=64×64, flip angle = 75°, slice thickness = 3.5mm, slice gap = 1.05 mm, field of view (FOV) 240 mm, matrix size = 64×64, voxel size = 3.75×3.75×4.55 mm<sup>3</sup>). **sMRI:** A multi-echo MPRAGE sequence was used with the following parameters: TR/TE/TI = 2530/[1.64, 3.5, 5.36, 7.22, 9.08]/900 ms, flip angle = 7°, FOV = 256×256 mm, slab thickness = 176 mm, matrix size= 256×256×176, Voxel size =1×1×1 mm, Pixel bandwidth =650 Hz, Total scan time = 6 min. **dMRI:** data was collected along the AC/PC line, throughout the whole brain, FOV= 256×256 mm, slice thickness = 2 mm, NEX (number of excitations) = 1, TE= 84 ms, TR= 9000ms. A multiple channel radio frequency coil was used, with GRAPPA (generalized auto calibrating partially parallel acquisition) (×2), 35 gradient directions, b = 800s/mm<sup>2</sup> and 5 measurements with b = 0. All images were registered to the first b = 0 image by FLIRT (FMRIB's Linear Image Registration Tool).

## Data Preprocessing

**fMRI:** SPM8 software package (<http://www.fil.ion.ucl.ac.uk/spm/software/spm8>) was employed to perform fMRI preprocessing. Slice timing was performed with the middle slice as the reference frame. Images were realigned using INRIalign (14). The fMRI data were then despiked to mitigate the impact of outliers and spatially normalized into the standard Montreal Neurological Institute (MNI) space (15) with slightly up-sampled to 3×3×3 mm<sup>3</sup>. We further regressed out 6 motion parameters, white matter and cerebrospinal fluid in denoising, the mean framewise displacements showed no significant group difference (meanFD, mean of root of mean square frame-to-frame head motions assuming 50 mm head radius (16); HC: 0.224±0.12mm, SZ:0.227±0.12mm,  $p=0.91$ ). Finally, data were spatially smoothed with a Gaussian kernel with FWHM of 8×8×8 mm<sup>3</sup>. For the rest-fMRI, we extracted the voxel-wise fractional ALFF (fALFF) to generate a map for each subject as did in (7, 17–19).

**dMRI** data were preprocessed by FMRIB Software Library (FSL; [www.fmrib.ox.ac.uk/fsl](http://www.fmrib.ox.ac.uk/fsl)) and consisted of the following steps: (a) quality check, any gradient directions with excessive motion or vibration artifacts were identified and removed; (b) motion and eddy current correction; (c) correction of gradient directions for any image rotation done during the previous motion correction step; (d) calculation of diffusion tensor and scalar measures such as FA, which were then smoothed, see more details in (20).

**sMRI** data were also preprocessed using the SPM8 software package which was used to segment the brain into white matter (WM), gray matter (GM), and cerebral spinal fluid with unmodulated normalized parameters via the unified segmentation method (21). Then the

GM images were smoothed to a full-width half maximum Gaussian kernel of 8mm (22). Subject outlier detection was further performed using a spatial Pearson correlation with the template image, to ensure that all subjects were properly segmented, for details, see (23).

**Normalization**—After preprocessing, the 3D brain images of each subject were reshaped into a one-dimensional vector and stacked, forming a matrix ( $N_{\text{subj}} \times N_{\text{voxel}}$ ) for each of the 3 modalities. These 3 matrices were then normalized to have the same average sum-of-squares (computed across all subjects and all voxels/locus for each modality) to ensure all modalities had the same ranges.

## Fusion Analysis

The preprocessed data were jointly analyzed by multi-set canonical correlation analysis (MCCA) (24), which enables assessment of linked alterations among three modalities and has been successfully applied to discriminate psychotic disorders (25, 26). Please see supplementary file for more details about MCCA and fusion methods selection. For fusion purpose, each modality is first reduced to a “feature” for each subject, providing a more tractable space to link the data (27). Here we used the fALFF maps (fMRI) (19), segmented GM images (sMRI), and FA maps (dMRI) as fusion input, as previously (7). As shown in Figure 1, MCCA jointly decomposes 3 datasets into mixing coefficients (matrices  $\mathbf{A}_k$ ) and components ( $\mathbf{C}_k$ , spatial maps,  $k$  is modality,  $k=1,2,3$ ), by which any pair-wise modality correlation between  $\mathbf{A}_i$  and  $\mathbf{A}_j$  ( $i, j$ ) are maximized and sorted from high to low. Consequently, the corresponding columns of  $\mathbf{A}_k$ , also called canonical variants (CVs), are linked among modalities and can be used to evaluate relationships with MCCB scores and to detect group differences. Their associated brain maps further demonstrate multimodal alterations that vary similarly across all subjects. Before MCCA, the factor of sex was regressed out to remove the potential influence of sex differences between groups. We choose 20 as the number of CVs based on the minimum description length (28) and more than 99.5% of the variance was retained for all three modalities.

## Correlation Analysis and Group Difference Detection

Correlation analyses were tested between each CV and MCCB scores (composite and specific domains), as well as PANSS scores. Two-sample t-tests were also performed between patients and controls for each CV, which of the same indices if showing group difference in all modalities, are called joint group-discriminative CVs that could indicate linked functional-structural alterations.

## RESULTS

### Joint components of interests

We aimed to investigate the joint components significantly related to MCCB and HC-SZ discrimination across 3 modalities. Among the 20 derived canonical variants, the 8<sup>th</sup> CV were found not only significantly group-discriminating ( $p=0.006, 0.008, 0.0009$  for fMRI, dMRI and sMRI respectively, FDR corrected for multiple comparison), but also correlated with MCCB composite ( $R=0.275, 0.215, 0.258$  for fMRI, dMRI and sMRI, respectively) and PANSS negative scores ( $R=-0.395, -0.287$  for fMRI and dMRI). No significant

correlation was found with medication using the olanzapine equivalent (29). As displayed in Figure 2, the spatial maps were transformed into Z values, visualized at  $|Z| > 2$  in Fig 2 (A) and adjusted as HC>SZ for all modalities on the mean of loading parameters, as the box plot shown in Fig 2 (B), so that the positive Z-values (red regions) indicate higher contribution in HC than SZ, and the negative Z-values (blue regions) indicate higher contribution in SZ than HC. The identified regions in CV8 are summarized in Table 2, for fALFF components (Talairach labels), FA (WM tracts, from John Hopkins Atlas) and GM (MNI labels) respectively. Fig 2 (C) indicates the positive correlation between loadings of CV8 in 3 modalities and the MCCB composite (HC: red dots, SZ: blue dots); the higher loadings correspond to better cognitive performance.

Common in fMRI\_CV8 and sMRI\_CV8, schizophrenia patients show lower values in sub-cortical regions including thalamus, striatum, hippocampus, parahippocampal gyrus and visual cortex (Brodmann area [BA] 18,19) than controls, but have higher contribution in intraparietal sulcus (IPS), which is part of the attention network. For fMRI only, patients indicate higher fALFF values in inferior parietal lobule (IPL), DLPFC, left middle temporal gyrus (MTG), and posterior part of Wernicke's area (BA 39,40). For GM only, patients are lower in somatosensory cortex, anterior cingulate cortex (ACC), DLPFC and anterior part of Wernicke's area (BA 22). These above regions can be viewed as part of a cortico-striato-thalamic loop. For dMRI, the co-occurring FA values in anterior thalamic radiation (ATR), superior longitudinal fasciculus (SLF) and cortico-spinal tract (CST) are lower in SZ, but higher in forceps major (FMAJ), inferior longitudinal fasciculus (ILF) and inferior frontal-occipital fasciculus (IFO).

Furthermore, CV8 also significantly correlated with some of the MCCB domain scores, as listed in Table 3. While fMRI\_CV8 and sMRI\_CV8 each correlate with 5 specific domains, all 3 modalities indicate significant correlation with the domain of social cognition ( $R=0.367, 0.243, 0.238$  for fMRI, dMRI and sMRI, respectively), suggesting that joint CV8 express a brain network that reflects comprehensive cognitive deficits in SZ, especially social cognition. In addition, a significant negative association was observed between fMRI\_CV8 loadings and PANSS negative scores ( $R=-0.395, p=0.006$ , FDR corrected). dMRI\_CV8 was at the fringe of the statistical significance ( $R=-0.285, p=0.05$ ). No significant correlation was found with PANSS positive scores.

### Multimodal co-alterations related to MCCB

Figure 3 displays the overlapped GM-FA and fALFF-FA spatial maps for visualizing co-occurring multimodal abnormalities specifically related to cognitive deficits, *i.e.*, changes in one modality (*e.g.* WM tract in red) associate with alterations in distant, but connected regions in another modality (*e.g.*, GM in green and fALFF in blue). In both cases, a cortico-striato-thalamic network covaries with FA in SLF, ATR and CST, whereas the fMRI alterations in hippocampus and parahippocampal gyrus are linked to mid-occipital gyrus and IPL through FMAJ and IFO.

## DISCUSSION

To our knowledge, this is the first study to investigate the interrelationships between MCCB, a comprehensive cognition measure for schizophrenia, and the abnormalities seen in three MRI modalities via a multivariate method. We found that: 1) the aberrant brain networks related to schizophrenia cognitive deficits are mainly in cortico-striato-thalamic circuits. 2) The identified functional or structural regions could well explain the MCCB domains correlated with each single modality respectively, as shown in Figure 4. Overall, these findings suggest that three-way fusion takes account of more relevant information to quantify the group differences and multimodal brain co-alterations.

### Co-alterations in cortico-striato-thalamic circuits

Figure 4 illustrates the covaried cortical maps of fMRI\_CV8 and sMRI\_CV8, and the summary of modality-specific networks correlated with individual MCCB domains. Each of the 3 components correlates with MCCB composite and social cognition, corresponding to the co-altered brain regions in the top row. Namely, the better cognitive performance, the higher fALFF (intensity of regional spontaneous brain activity) or GM volumes are in subcortical areas (thalamus, striatum, hippocampus) and the mid-occipital regions. Similar findings were verified in resting-state fMRI studies in (30) (31). The DLPFC were also co-involved with higher fALFF values but lower GM volume in schizophrenia, supported by (32–34). The above regions are part of a cortical-striato-thalamic loop as described in (35): The striatum, comprising the caudate and putamen, receives inputs from cortex, thalamus, hippocampus, and amygdala; it projects its output structures to thalamus; the thalamus finally projects back to the cortex, thereby completing a circuit (36, 37).

In this circuit, thalamus is believed to act as a relay station between many subcortical areas and the cerebral cortex (38) and has multiple functions, *e.g.*, coordinating, encoding, retrieval, and planning (39). Our results are consistent with a previous report (40) in which schizophrenia patients exhibited decreased fMRI thalamic activation and showed significant positive correlation between working memory performance and thalamic functional activation (41). The striatum has a role in the planning and some executive functions. As reviewed in (37), the striatum and its cortical connections are critical for complex cognition, and the altered striatal activity could indirectly change cortical functioning via the thalamus. Other reports (42) also suggested lesions of the striatum or its associative loops affect various attentional and cognitive control processes. For hippocampus, previous work has found that SZ patients with poorer working memory performance exhibited reduced hippocampal GM volume (43) and higher intrinsic hippocampal activity (3) as we did.

Other commonly detected regions in fMRI and sMRI include lingual gyrus and parahippocampal gyrus, which play important roles in visual memory encoding and word recognition specifically (44), which are involved in 7 of the 10 MCCB tasks. Coincidentally, both fALFF\_CV8 and GM\_CV8 correlate with domains of “processing speed” and “attention/vigilance”. Combined with findings in Fig 3 where FMAJ and IFO co-occurring in FA, supporting that the impaired visual memory/attention in schizophrenia is related to either dysfunction of mid-occipital regions or disconnections between them and other brain structures (45, 46). In addition, part of the salience network, including anterior cingulate

cortex (ACC) and insula, was detected in GM, which is involved in a variety of monitoring, attention switching, and decision-making processes (47), in accordance with the domains correlated with sMRI.

Figure 3 further illustrates the modality-spanning co-alterations across 3 modalities. Given the current literature on the neurophysiology of the relevant brain regions (7, 37, 39, 48) and the discovered MCCB correlations, we posit that schizophrenia patients may have abnormalities in the modulation circuit connecting striatum to frontal-parietal-occipital function via the thalamus. (49). In studies of cognitive impairment, the sub-cortical and parietal-occipital regions usually received less attention compared to prefrontal cortex (50). Our findings suggest that it is the cortico-striato-thalamic loop critical for complex cognition, which are anatomical substrates for many motor and executive functions and social cognition. This is consistent with the hypothesis that a disruption in this loop may lead to an impairment in synchrony or smooth coordination of mental processes (51), accounting for the wide range of cognitive deficits (49, 52) and is implicated in diverse neuropsychiatric disorders (53–55).

### Particular brain regions associated with specific MCCB domains

The identified modality-specific brain patterns correspond to their associated domains as well. For instance, the domains of “visual learning” and “verbal learning” only correlate with fMRI\_CV8, where posterior Wernicke’s area (BA 39,40 (56)), IPL, left MTG were uniquely found in fMRI. Wernicke’s area had been accepted as specialized in language comprehension and word generation/understanding (57, 58), while regional ALFF value from the left MTG was found highly correlated with semantic processing efficiency in HC (59); both of them corresponded to verbal learning domain here. In addition, IPL especially angular gyrus (AG) had shown strong involvement in semantic processing, social cognition or theory-of-mind in several meta-analysis reviews (60–62); coincidentally, fMRI\_CV8 has the highest correlation with social cognition among all correlations ( $R=0.367$ ,  $p=0.0003$ , FDR corrected): the higher fALFF in AG, the poorer social cognition with participants, in agreement with (63).

By contrast, the domains of “reasoning” and “working memory” are only correlated with sMRI, in accordance with executive control networks detected only in sMRI, *i.e.*, DLPFC and left STG, where SZ patients showed reduced GM volume and lower domain scores. DLPFC was involved in executive function (2), as well as working memory in fMRI studies (64, 65). It’s also frequently involved in planning and decision making (66), corresponding to the reasoning task—maze in MCCB (67). Consistent with our findings, Hazlett (68) reported larger BA10 volume in DLPFC could predict less symptom severity in schizotypal personality disorder; while Kawada (69) found executive dysfunction scores were correlated with volume reduction in DLPFC in schizophrenia. Similarly, the posterior left STG (BA 22), which responded to external sources of speech and words (56), appeared to be central to the acquisition of long-term lexical memories. Its GM volume was found to be correlated with the severity of thought disorder (70) and auditory hallucinations (71). Hence, the identified GM-specific changes could well explain the MCCB domains uniquely associated with sMRI.



Finally, both fMRI\_CV8 and dMRI\_CV8 inversely correlate with PANSS negative scores, which share many features with cognitive impairment (72, 73), suggesting the affected regions shown in fALFF\_FA may function in concert to mediate various executive functions (50), which also underlie the negative symptom construct of schizophrenia (37, 74). Regarding dMRI findings, both decreased and increased FA values in SZ were found in our study as listed in Table 2. The identified regions with reduced FA values are consistent with most dMRI studies in schizophrenia (48, 75). Nevertheless, a few studies also reported some focal increased FA as exemplified in the networks underlying symptoms such as hallucinations and delusions (76, 77), especially in the inter-hemispheric and cortico-cortical WM connections. For example, (78) found a very similar pattern of FA increases in the forceps major as we did. (79) also reported FA increases on ILF and IFO tracts in schizophrenia patients, whose FA values were initially lower than controls before being treated by olanzapine. Therefore, the pathophysiologic reasons of increased FA in schizophrenia can be complex and diverse (76): it may depend on the developmental stage of the patients (80) and exposure to antipsychotic medications (79), which may potentially impact on our results.

### Aspects of multimodal fusion

Basically, the joint analysis of resting-state fMRI, dMRI, sMRI and their associations with MCCB support brain function as comprised of multiple, distinct, and interacting networks. This allowed us to discover multimodal co-alterations related to fundamental aspects of cognitive impairment in schizophrenia, which cannot be easily captured by separate analysis of each single modality. The findings that linked multimodal changes include both increased and decreased effects on MCCB performance, suggest that the relationship between pathology in cortico-striato-thalamic circuits and the associated "cognitive dysmetria" (39) in schizophrenia is complex. It is also important to emphasize that though MCCA can identify covarying multimodal components, it cannot itself answer the question of why the relevant modality-spanning features co-occur, but there may be two possible reasons. First, the co-occurrence of structural and functional features might be due to direct causal influences between them. For example, a disrupted WM tract could affect the regions it connects. Another explanation is both structural and functional abnormalities might be co-manifestations of an underlying common disease construct. Future studies with refined WM tractography or neuroanatomy-based approaches may further elaborate these possibilities. More tentatively, these results invite further investigation into avenues for exploring multimodal biomarkers of other measures of interest (*e.g.*, Glutamine/Glutamate metabolism) for several brain disorders, as did in (25).

### Potential limitations and future directions

In order to fully evaluate the multimodal variations in the cortico-striato-thalamic loop as a biomarker of MCCB, additional longitudinal research with symptoms tracking spaced sufficiently far apart during disease progression are needed. We plan to pursue this approach. In addition, the assumption here is that the correlation trends between the imaging maps and MCCB scores would be similar in both groups, in consistent with (81, 82), whereas our method also allows patients and controls to exhibit opposite correlations between imaging signatures and cognition by separately calculating correlations within each

group, as shown in (83). In future studies with more subjects and greater statistical power or with task-related fMRI, we may expect to find such relationships. Another problem is that SZ and HC were not perfectly sex-matched in current study and one cognitive domain (Attention/ Vigilance) was sex-related ( $r=0.205$ ,  $p=0.045$ )., Though we regressed sex effects, future studies need to consider this potential confound. In addition, though no direct correlation was found between antipsychotic dose and the identified component, the medication may still have an underlying effect on multimodal imaging measures of the schizophrenia patients, as previously reported on fALFF (84), DTI (85), and gray matter (86). Our future work also plans to utilize multimodal brain imaging features to predict cognitive/ symptom scores in patients, which is consistent with the initiative of NIH Research Domain Criteria (RDoC) project that intends to classify mental disorders based on dimensions of observable behavior and neurobiological measures.

In summary, this is the first study to use a multivariate, multimodal methodology to investigate neuroimaging correlates of MCCB in schizophrenia. Our results support the view that linked functional and structural deficits in distributed cortico-striato-thalamic circuit may account for several aspects of cognitive impairment in schizophrenia. We also identified focal deficits in a single modality that may relate to a specific domain, *e.g.*, the increased fALFF values in IPL significantly correlate with declined social cognition (87), suggesting that distinct dimensional aspects of MCCB might exhibit dissociable multimodal imaging signatures. Finally, based on the above results, we suggest that treatment strategies targeting thalamic and striatal (37) regulation of frontal-parietal-occipital networks may result in cognitive improvement in schizophrenia.

## Supplementary Material

Refer to Web version on PubMed Central for supplementary material.

## ACKNOWLEDGMENT

This work was supported by the National Institutes of Health grants R01MH084898 (to Bustillo J); R01EB 006841, R01EB 005846, and 5P20RR021938 (to Calhoun VD); “100 Talents Plan” of Chinese Academy of Sciences, the State High-Tech Development Plan (863) (Grant No. SQ2015AA0200506) and Chinese National Science Foundation No. 81471367 (to J. Sui); and the Strategic Priority Research Program of the Chinese Academy of Sciences (Grant No. SQ2015AA02030300) and National Key Basic Research and Development (973) (Grant No. 2011CB707800) (to T. Jiang).

## REFERENCES

1. Green MF, Kern RS, Heaton RK. Longitudinal studies of cognition and functional outcome in schizophrenia: implications for MATRICS. *Schizophrenia research*. 2004; 72:41–51. [PubMed: 15531406]
2. Chan RC, Shum D, Touloupoulou T, Chen EY. Assessment of executive functions: review of instruments and identification of critical issues. *Arch Clin Neuropsychol*. 2008; 23:201–216. [PubMed: 18096360]
3. Tregellas JR, Smucny J, Harris JG, Olincy A, Maharajh K, Kronberg E, et al. Intrinsic Hippocampal Activity as a Biomarker for Cognition and Symptoms in Schizophrenia. *The American journal of psychiatry*. 2014
4. Rissling AJ, Makeig S, Braff DL, Light GA. Neurophysiologic markers of abnormal brain activity in schizophrenia. *Curr Psychiatry Rep*. 2010; 12:572–578. [PubMed: 20857348]

5. August SM, Kiwanuka JN, McMahon RP, Gold JM. The MATRICS Consensus Cognitive Battery (MCCB): clinical and cognitive correlates. *Schizophrenia research*. 2011; 134:76–82. [PubMed: 22093182]
6. Stephen JM, Coffman BA, Jung RE, Bustillo JR, Aine CJ, Calhoun VD. Using joint ICA to link function and structure using MEG and DTI in schizophrenia. *NeuroImage*. 2013; 83:418–430. [PubMed: 2377757]
7. Sui J, He H, Yu Q, Chen J, Rogers J, Pearlson GD, et al. Combination of Resting State fMRI, DTI, and sMRI Data to Discriminate Schizophrenia by N-way MCCA + jICA. *Front Hum Neurosci*. 2013; 7:235. [PubMed: 23755002]
8. First, MB.; Spitzer, RL.; Gibbon, M.; Williams, JB. Structured Clinical Interview for DSM-IV axis I disorders. patient edition (SCID-I/P, Version 2.0) ed. New York: Biometrics Research Department, New York State Psychiatric Institute; 1995.
9. Kay SR, Fiszbein A, Opler LA. The positive and negative syndrome scale (PANSS) for schizophrenia. *Schizophr Bull*. 1987; 13:261–276. [PubMed: 3616518]
10. Nuechterlein KH, Green MF, Kern RS, Baade LE, Barch DM, Cohen JD, et al. The MATRICS Consensus Cognitive Battery, part 1: test selection, reliability, and validity. *The American journal of psychiatry*. 2008; 165:203–213. [PubMed: 18172019]
11. Kern RS, Nuechterlein KH, Green MF, Baade LE, Fenton WS, Gold JM, et al. The MATRICS Consensus Cognitive Battery, part 2: co-norming and standardization. *The American journal of psychiatry*. 2008; 165:214–220. [PubMed: 18172018]
12. Siu CO. Interpreting T scores and percentile equivalents using the MATRICS consensus cognitive battery in schizophrenia trials. *The American journal of psychiatry*. 2008; 165:914. author reply 914–915. [PubMed: 18593789]
13. Burton CZ, Vella L, Harvey PD, Patterson TL, Heaton RK, Twamley EW. Factor structure of the MATRICS Consensus Cognitive Battery (MCCB) in schizophrenia. *Schizophrenia research*. 2013; 146:244–248. [PubMed: 23507359]
14. Freire L, Roche A, Mangin JF. What is the best similarity measure for motion correction in fMRI time series? *IEEE Trans Med Imaging*. 2002; 21:470–484. [PubMed: 12071618]
15. Friston KJ, Ashburner J, Frith CD, Poline JP, Heather JD, Frackowiak RS. Spatial registration and normalization of images. *Hum Brain Mapp*. 1995; 2:165–189.
16. Allen EA, Erhardt EB, Damaraju E, Gruner W, Segall JM, Silva RF, et al. A baseline for the multivariate comparison of resting-state networks. *Front Syst Neurosci*. 2011; 5:2. [PubMed: 21442040]
17. Erhardt EB, Allen EA, Damaraju E, Calhoun VD. On network derivation, classification, and visualization: a response to Habeck and Moeller. *Brain Connect*. 2011; 1:1–19. [PubMed: 21808745]
18. Calhoun VD, Allen E. Extracting Intrinsic Functional Networks with Feature-based Group Independent Component Analysis. *Psychometrika*. 2012:1–17. in press.
19. Zou QH, Zhu CZ, Yang Y, Zuo XN, Long XY, Cao QJ, et al. An improved approach to detection of amplitude of low-frequency fluctuation (ALFF) for resting-state fMRI: fractional ALFF. *J Neurosci Methods*. 2008; 172:137–141. [PubMed: 18501969]
20. Sui J, Pearlson G, Caprihan A, Adali T, Kiehl KA, Liu J, et al. Discriminating schizophrenia and bipolar disorder by fusing fMRI and DTI in a multimodal CCA+ joint ICA model. *NeuroImage*. 2011; 57:839–855. [PubMed: 21640835]
21. Ashburner J, Friston KJ. Unified segmentation. *NeuroImage*. 2005; 26:839–851. [PubMed: 15955494]
22. White T, O'Leary D, Magnotta V, Arndt S, Flaum M, Andreasen NC. Anatomic and functional variability: the effects of filter size in group fMRI data analysis. *NeuroImage*. 2001; 13:577–588. [PubMed: 11305887]
23. Segall JM, Turner JA, van Erp TG, White T, Bockholt HJ, Gollub RL, et al. Voxel-based morphometric multisite collaborative study on schizophrenia. *Schizophr Bull*. 2009; 35:82–95. [PubMed: 18997157]
24. Li YO, Adali T, Wang W, Calhoun VD. Joint Blind Source Separation by Multi-set Canonical Correlation Analysis. *IEEE Trans Signal Process*. 2009; 57:3918–3929. [PubMed: 20221319]

25. Sui J, He H, Pearlson GD, Adali T, Kiehl KA, Yu Q, et al. Three-way (N-way) fusion of brain imaging data based on mCCA+jICA and its application to discriminating schizophrenia. *NeuroImage*. 2012; 2:119–132. [PubMed: 23108278]
26. Correa NM, Li YO, Adali T, Calhoun VD. Canonical Correlation Analysis for Feature-Based Fusion of Biomedical Imaging Modalities and Its Application to Detection of Associative Networks in Schizophrenia. *IEEE J Sel Top Signal Process*. 2008; 2:998–1007. [PubMed: 19834573]
27. Smith SM, Fox PT, Miller KL, Glahn DC, Fox PM, Mackay CE, et al. Correspondence of the brain's functional architecture during activation and rest. *Proceedings of the National Academy of Sciences of the United States of America*. 2009; 106:13040–13045. [PubMed: 19620724]
28. Li YO, Adali T, Calhoun VD. Estimating the number of independent components for functional magnetic resonance imaging data. *Hum Brain Mapp*. 2007; 28:1251–1266. [PubMed: 17274023]
29. Gardner DM, Murphy AL, O'Donnell H, Centorrino F, Baldessarini RJ. International consensus study of antipsychotic dosing. *The American journal of psychiatry*. 2010; 167:686–693. [PubMed: 20360319]
30. Huang XQ, Lui S, Deng W, Chan RC, Wu QZ, Jiang LJ, et al. Localization of cerebral functional deficits in treatment-naive, first-episode schizophrenia using resting-state fMRI. *NeuroImage*. 2010; 49:2901–2906. [PubMed: 19963069]
31. Hoptman MJ, Zuo XN, Butler PD, Javitt DC, D'Angelo D, Mauro CJ, et al. Amplitude of low-frequency oscillations in schizophrenia: a resting state fMRI study. *Schizophrenia research*. 2010; 117:13–20. [PubMed: 19854028]
32. Gur RE, Cowell PE, Latshaw A, Turetsky BI, Grossman RI, Arnold SE, et al. Reduced dorsal and orbital prefrontal gray matter volumes in schizophrenia. *Arch Gen Psychiatry*. 2000; 57:761–768. [PubMed: 10920464]
33. Turner JA, Damaraju E, van Erp TG, Mathalon DH, Ford JM, Voyvodic J, et al. A multisite resting state fMRI study on the amplitude of low frequency fluctuations in schizophrenia. *Front Neurosci*. 2013; 7:137. [PubMed: 23964193]
34. Potkin SG, Turner JA, Brown GG, McCarthy G, Greve DN, Glover GH, et al. Working memory and DLPFC inefficiency in schizophrenia: the FBIRN study. *Schizophr Bull*. 2009; 35:19–31. [PubMed: 19042912]
35. Kegeles LS, Frankle WG, Gil R, Narendran R, Slifstein M, Hwang DR, Cangiano C, Haber SN, Abi-Dargham A, Laruelle MC. Schizophrenia is associated with increased synaptic dopamine in associative rather than limbic regions of the striatum: implications for mechanisms of action of antipsychotic drugs. *J Nucl Med*. 2006; 47:139.
36. Alexander GE, DeLong MR, Strick PL. Parallel organization of functionally segregated circuits linking basal ganglia and cortex. *Annu Rev Neurosci*. 1986; 9:357–381. [PubMed: 3085570]
37. Simpson EH, Kellendonk C, Kandel E. A possible role for the striatum in the pathogenesis of the cognitive symptoms of schizophrenia. *Neuron*. 2010; 65:585–596. [PubMed: 20223196]
38. Andreasen NC. The role of the thalamus in schizophrenia. *Canadian journal of psychiatry*. 1997; 42:27–33.
39. Andreasen NC, Paradiso S, O'Leary DS. "Cognitive dysmetria" as an integrative theory of schizophrenia: a dysfunction in cortical-subcortical-cerebellar circuitry? *Schizophr Bull*. 1998; 24:203–218. [PubMed: 9613621]
40. Andrews J, Wang L, Csernansky JG, Gado MH, Barch DM. Abnormalities of thalamic activation and cognition in schizophrenia. *The American journal of psychiatry*. 2006; 163:463–469. [PubMed: 16513868]
41. Danos P. Pathology of the thalamus and schizophrenia--an overview. *Fortschr Neurol Psychiatr*. 2004; 72:621–634. [PubMed: 15529234]
42. Chudasama Y, Robbins TW. Functions of frontostriatal systems in cognition: comparative neuropsychopharmacological studies in rats, monkeys and humans. *Biol Psychol*. 2006; 73:19–38. [PubMed: 16546312]
43. Wexler BE, Zhu H, Bell MD, Nicholls SS, Fulbright RK, Gore JC, et al. Neuropsychological near normality and brain structure abnormality in schizophrenia. *The American journal of psychiatry*. 2009; 166:189–195. [PubMed: 18765481]

44. Mechelli A, Humphreys GW, Mayall K, Olson A, Price CJ. Differential effects of word length and visual contrast in the fusiform and lingual gyri during reading. *Proceedings Biological sciences / The Royal Society*. 2000; 267:1909–1913. [PubMed: 11052544]
45. Palaniyappan L, Al-Radaideh A, Mougín O, Gowland P, Liddle PF. Combined white matter imaging suggests myelination defects in visual processing regions in schizophrenia. *Neuropsychopharmacology*. 2013; 38:1808–1815. [PubMed: 23558741]
46. Ragland JD, Moelter ST, Bhati MT, Valdez JN, Kohler CG, Siegel SJ, et al. Effect of retrieval effort and switching demand on fMRI activation during semantic word generation in schizophrenia. *Schizophrenia research*. 2008; 99:312–323. [PubMed: 18155880]
47. Menon V, Uddin LQ. Saliency, switching, attention and control: a network model of insula function. *Brain Struct Funct*. 2010; 214:655–667. [PubMed: 20512370]
48. Kubicki M, McCarley R, Westin CF, Park HJ, Maier S, Kikinis R, et al. A review of diffusion tensor imaging studies in schizophrenia. *J Psychiatr Res*. 2007; 41:15–30. [PubMed: 16023676]
49. Pantelis C, Barnes TR, Nelson HE, Tanner S, Weatherley L, Owen AM, et al. Frontal-striatal cognitive deficits in patients with chronic schizophrenia. *Brain*. 1997; 120(10):1823–1843. [PubMed: 9365373]
50. engör NS, Karabacak O, Steinmetz U. A Computational Model of Cortico-Striato-Thalamic Circuits in Goal-Directed Behaviour. *International Conference of Artificial Neural Networks - ICANN 2008*. 2008; 5164:328–337.
51. Stocco A, Lebiere C, Anderson JR. Conditional routing of information to the cortex: a model of the basal ganglia's role in cognitive coordination. *Psychological review*. 2010; 117:541–574. [PubMed: 20438237]
52. Graybiel AM, Rauch SL. Toward a neurobiology of obsessive-compulsive disorder. *Neuron*. 2000; 28:343–347. [PubMed: 11144344]
53. Honey GD, Suckling J, Zelaya F, Long C, Routledge C, Jackson S, et al. Dopaminergic drug effects on physiological connectivity in a human cortico-striato-thalamic system. *Brain*. 2003; 126:1767–1781. [PubMed: 12805106]
54. Alexander GE, Crutcher MD, DeLong MR. Basal ganglia-thalamocortical circuits: parallel substrates for motor, oculomotor, "prefrontal" and "limbic" functions. *Prog Brain Res*. 1990; 85:119–146. [PubMed: 2094891]
55. Masterman DL, Cummings JL. Frontal-subcortical circuits: the anatomic basis of executive, social and motivated behaviors. *J Psychopharmacol*. 1997; 11:107–114. [PubMed: 9208374]
56. Wise RJ, Scott SK, Blank SC, Mummery CJ, Murphy K, Warburton EA. Separate neural subsystems within 'Wernicke's area'. *Brain*. 2001; 124:83–95. [PubMed: 11133789]
57. DeWitt I, Rauschecker JP. Wernicke's area revisited: parallel streams and word processing. *Brain Lang*. 2013; 127:181–191. [PubMed: 24404576]
58. Ross ED. Cerebral localization of functions and the neurology of language: fact versus fiction or is it something else? *Neuroscientist*. 2010; 16:222–243. [PubMed: 20139334]
59. Wei T, Liang X, He Y, Zang Y, Han Z, Caramazza A, et al. Predicting conceptual processing capacity from spontaneous neuronal activity of the left middle temporal gyrus. *J Neurosci*. 2012; 32:481–489. [PubMed: 22238084]
60. Binder JR, Desai RH, Graves WW, Conant LL. Where is the semantic system? A critical review and meta-analysis of 120 functional neuroimaging studies. *Cereb Cortex*. 2009; 19:2767–2796. [PubMed: 19329570]
61. Mars RB, Jbabdi S, Sallet J, O'Reilly JX, Croxson PL, Olivier E, et al. Diffusion-weighted imaging tractography-based parcellation of the human parietal cortex and comparison with human and macaque resting-state functional connectivity. *J Neurosci*. 2011; 31:4087–4100. [PubMed: 21411650]
62. Seghier ML. The angular gyrus: multiple functions and multiple subdivisions. *Neuroscientist*. 2013; 19:43–61. [PubMed: 22547530]
63. Yu R, Chien YL, Wang HL, Liu CM, Liu CC, Hwang TJ, et al. Frequency-specific alternations in the amplitude of low-frequency fluctuations in schizophrenia. *Hum Brain Mapp*. 2014; 35:627–637. [PubMed: 23125131]

64. Manoach DS, Press DZ, Thangaraj V, Searl MM, Goff DC, Halpern E, et al. Schizophrenic subjects activate dorsolateral prefrontal cortex during a working memory task, as measured by fMRI. *Biological psychiatry*. 1999; 45:1128–1137. [PubMed: 10331104]
65. Kim DI, Manoach DS, Mathalon DH, Turner JA, Mannell M, Brown GG, et al. Dysregulation of working memory and default-mode networks in schizophrenia using independent component analysis, an fBIRN and MCIC study. *Hum Brain Mapp*. 2009
66. Rodriguez-Sanchez JM, Crespo-Facorro B, Perez-Iglesias R, Gonzalez-Blanch C, Alvarez-Jimenez M, Llorca J, et al. Prefrontal cognitive functions in stabilized first-episode patients with schizophrenia spectrum disorders: a dissociation between dorsolateral and orbitofrontal functioning. *Schizophrenia research*. 2005; 77:279–288. [PubMed: 15950437]
67. Plis SM, Sui J, Lane T, Roy S, Clark VP, Potluru VK, et al. High-order interactions observed in multi-task intrinsic networks are dominant indicators of aberrant brain function in schizophrenia. *NeuroImage*. 2013
68. Hazlett EA, Lamade RV, Graff FS, McClure MM, Kolaitis JC, Goldstein KE, et al. Visual-spatial working memory performance and temporal gray matter volume predict schizotypal personality disorder group membership. *Schizophrenia research*. 2014; 152:350–357. [PubMed: 24398009]
69. Kawada R, Yoshizumi M, Hirao K, Fujiwara H, Miyata J, Shimizu M, et al. Brain volume and dysexecutive behavior in schizophrenia. *Prog Neuropsychopharmacol Biol Psychiatry*. 2009; 33:1255–1260. [PubMed: 19625009]
70. Shenton ME, Kikinis R, Jolesz FA, Pollak SD, LeMay M, Wible CG, et al. Abnormalities of the left temporal lobe and thought disorder in schizophrenia. A quantitative magnetic resonance imaging study. *N Engl J Med*. 1992; 327:604–612. [PubMed: 1640954]
71. Barta PE, Pearlson GD, Powers RE, Richards SS, Tune LE. Auditory hallucinations and smaller superior temporal gyral volume in schizophrenia. *The American journal of psychiatry*. 1990; 147:1457–1462. [PubMed: 2221156]
72. Kirkpatrick B, Fenton WS, Carpenter WT Jr, Marder SR. The NIMH-MATRICES consensus statement on negative symptoms. *Schizophr Bull*. 2006; 32:214–219. [PubMed: 16481659]
73. Harvey PD, Koren D, Reichenberg A, Bowie CR. Negative symptoms and cognitive deficits: what is the nature of their relationship? *Schizophr Bull*. 2006; 32:250–258. [PubMed: 16221995]
74. Sergi MJ, Rassovsky Y, Widmark C, Reist C, Erhart S, Braff DL, et al. Social cognition in schizophrenia: relationships with neurocognition and negative symptoms. *Schizophrenia research*. 2007; 90:316–324. [PubMed: 17141477]
75. Lim KO, Helpert JA. Neuropsychiatric applications of DTI - a review. *NMR Biomed*. 2002; 15:587–593. [PubMed: 12489105]
76. Filippi M, Canu E, Gasparotti R, Agosta F, Valsecchi P, Lodoli G, et al. Patterns of brain structural changes in first-contact, antipsychotic drug-naive patients with schizophrenia. *Ajnr*. 2014; 35:30–37. [PubMed: 23744689]
77. Alba-Ferrara LM, de Erausquin GA. What does anisotropy measure? Insights from increased and decreased anisotropy in selective fiber tracts in schizophrenia. *Frontiers in integrative neuroscience*. 2013; 7:9. [PubMed: 23483798]
78. Wassermann D, Kanterakis E, Gur RC, Deriche R, Verma R. Diffusion-based population statistics using tract probability maps. *Med Image Comput Comput Assist Interv (MICCAI) Conference*. 2010; 13:631–639.
79. Ozelik-Eroglu E, Ertugrul A, Oguz KK, Has AC, Karahan S, Yazici MK. Effect of clozapine on white matter integrity in patients with schizophrenia: a diffusion tensor imaging study. *Psychiatry research*. 2014; 223:226–235. [PubMed: 25012780]
80. Samartzis L, Dima D, Fusar-Poli P, Kyriakopoulos M. White matter alterations in early stages of schizophrenia: a systematic review of diffusion tensor imaging studies. *J Neuroimaging*. 2014; 24:101–110. [PubMed: 23317110]
81. Whitfield-Gabrieli S, Thermenos HW, Milanovic S, Tsuang MT, Faraone SV, McCarley RW, et al. Hyperactivity and hyperconnectivity of the default network in schizophrenia and in first-degree relatives of persons with schizophrenia. *Proceedings of the National Academy of Sciences of the United States of America*. 2009; 106:1279–1284. [PubMed: 19164577]

82. Unschuld PG, Buchholz AS, Varvaris M, van Zijl PC, Ross CA, Pekar JJ, et al. Prefrontal brain network connectivity indicates degree of both schizophrenia risk and cognitive dysfunction. *Schizophr Bull.* 2014; 40:653–664. [PubMed: 23778975]
83. Falkenberg LE, Westerhausen R, Craven AR, Johnsen E, Kroken RA, EM LB, et al. Impact of glutamate levels on neuronal response and cognitive abilities in schizophrenia. *Neuroimage Clin.* 2014; 4:576–584. [PubMed: 24749064]
84. Hadley JA, Nenert R, Kraguljac NV, Bolding MS, White DM, Skidmore FM, et al. Ventral tegmental area/midbrain functional connectivity and response to antipsychotic medication in schizophrenia. *Neuropsychopharmacology.* 2014; 39:1020–1030. [PubMed: 24165885]
85. Szeszko PR, Robinson DG, Ikuta T, Peters BD, Gallego JA, Kane J, et al. White matter changes associated with antipsychotic treatment in first-episode psychosis. *Neuropsychopharmacology.* 2014; 39:1324–1331. [PubMed: 24549105]
86. Hutcheson NL, Clark DG, Bolding MS, White DM, Lahti AC. Basal ganglia volume in unmedicated patients with schizophrenia is associated with treatment response to antipsychotic medication. *Psychiatry research.* 2014; 221:6–12. [PubMed: 24210948]
87. Green MF, Bearden CE, Cannon TD, Fiske AP, Helleman GS, Horan WP, et al. Social cognition in schizophrenia, Part 1: performance across phase of illness. *Schizophr Bull.* 2012; 38:854–864. [PubMed: 21345917]

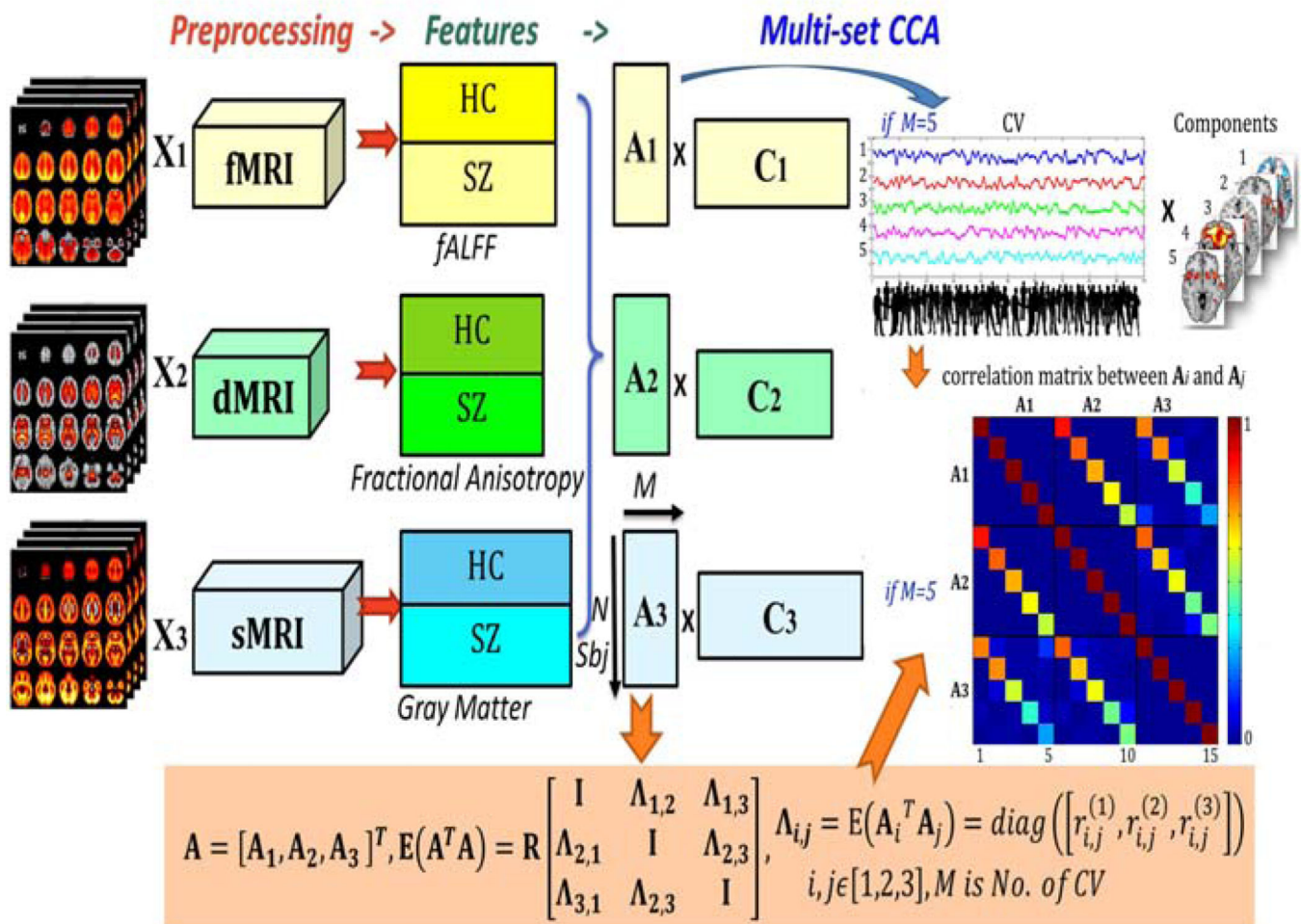


**Figure 1. Joint analysis flowchart of fMRI-dMRI-sMRI fusion based on MCCA**  
 Flowchart of fMRI-dMRI-sMRI fusion based on multi-set CCA, which enables identification of linked modality-spanning alterations. In our case, the feature matrix of each modality is decomposed as 20 canonical variants (CVs) and 20 corresponding spatial maps (components),  $M=20$ . The CV represents how the component is distributed in participants, which can be used to correlate with MCCB and symptom scores.



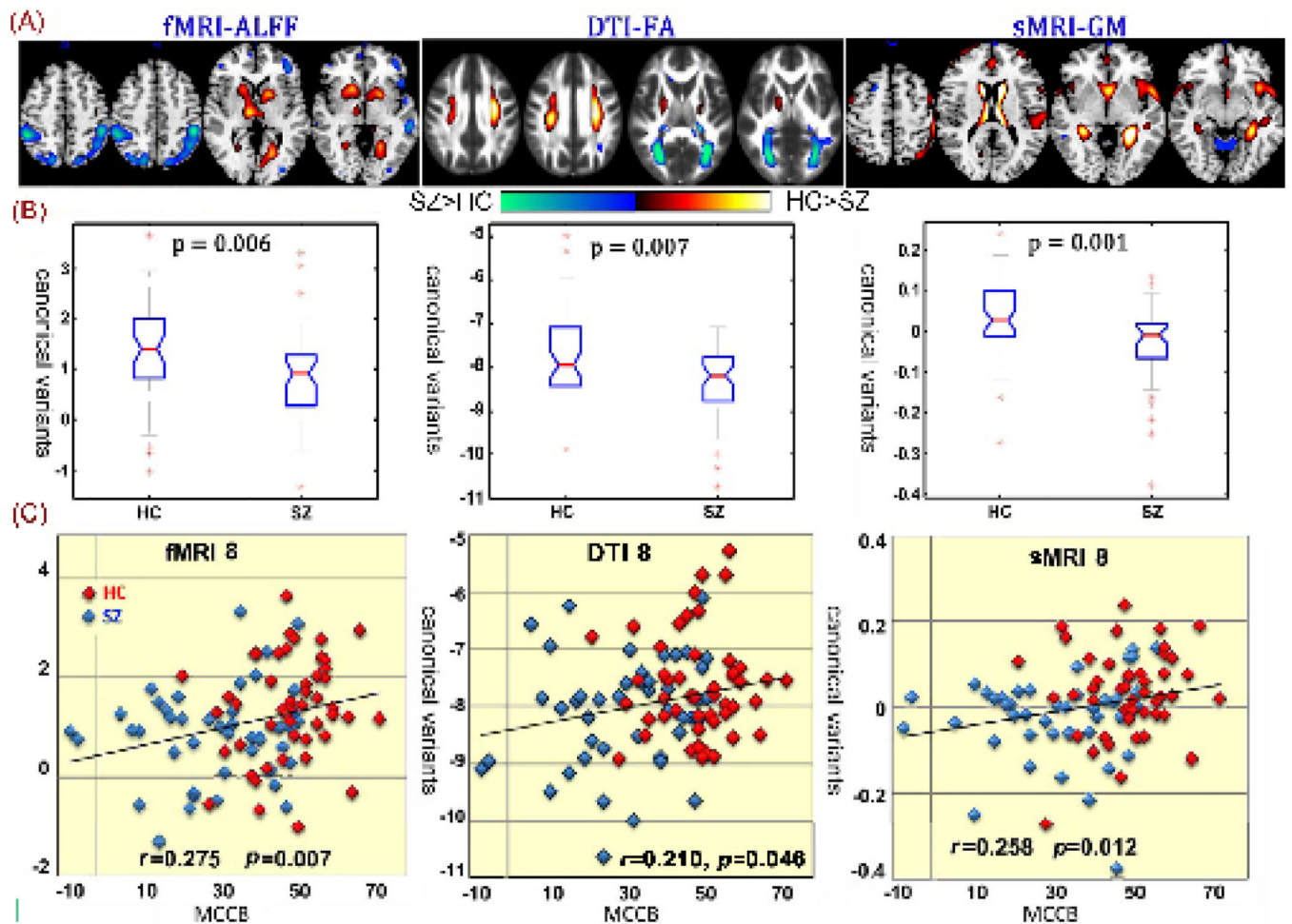


**Figure 2. Joint CV8 that correlated with MCCB composite scores in all modalities, and differed between groups**

Joint components that are significantly group-discriminating, also correlate with MCCB composite scores in all modalities. (A) The spatial maps visualized at  $|Z| > 2$ ; the positive Z-values (red regions) means HC > SZ and the negative Z-values (blue regions) means HC < SZ. (B) Boxplot of the loading parameters for each component, with the p values of two sample t-test between HC and SZ shown above. (C) Correlations between loadings of component and the MCCB composite scores (HC: red dots, SZ: blue dots); the higher loadings correspond to better cognitive performance.

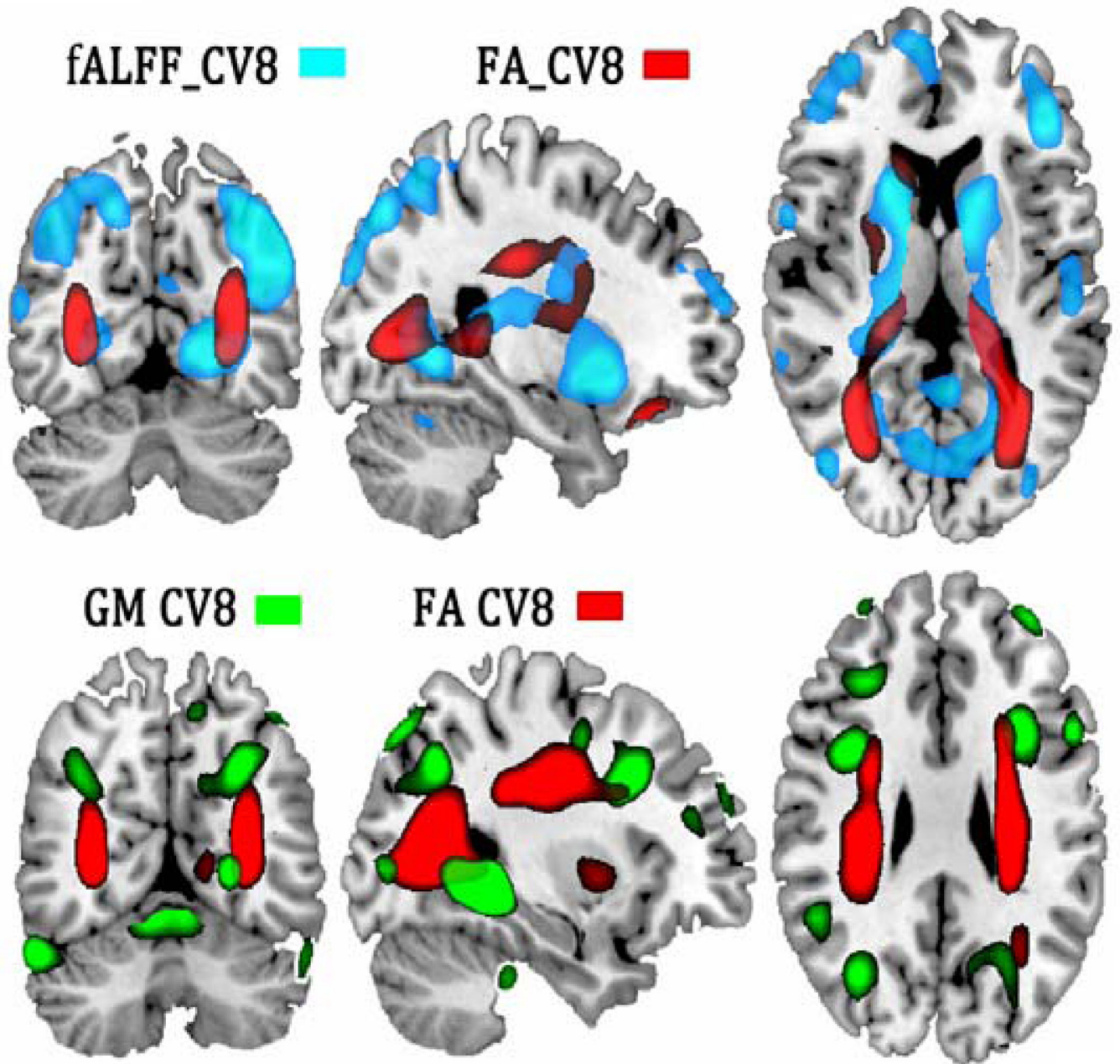


**Figure 3. Multimodal co-alterations manifested in GM-FA and fALFF-FA in CV8**

Multimodal co-alterations manifested between joint components, indicating changes in WM tracts (in red) associated with brain alterations in distant, but connected regions in GM (in green) or in fALFF (in blue). In both cases, a cortico-striato-thalamic network covaried with FA values in SLF, ATR, CST and FMAJ.

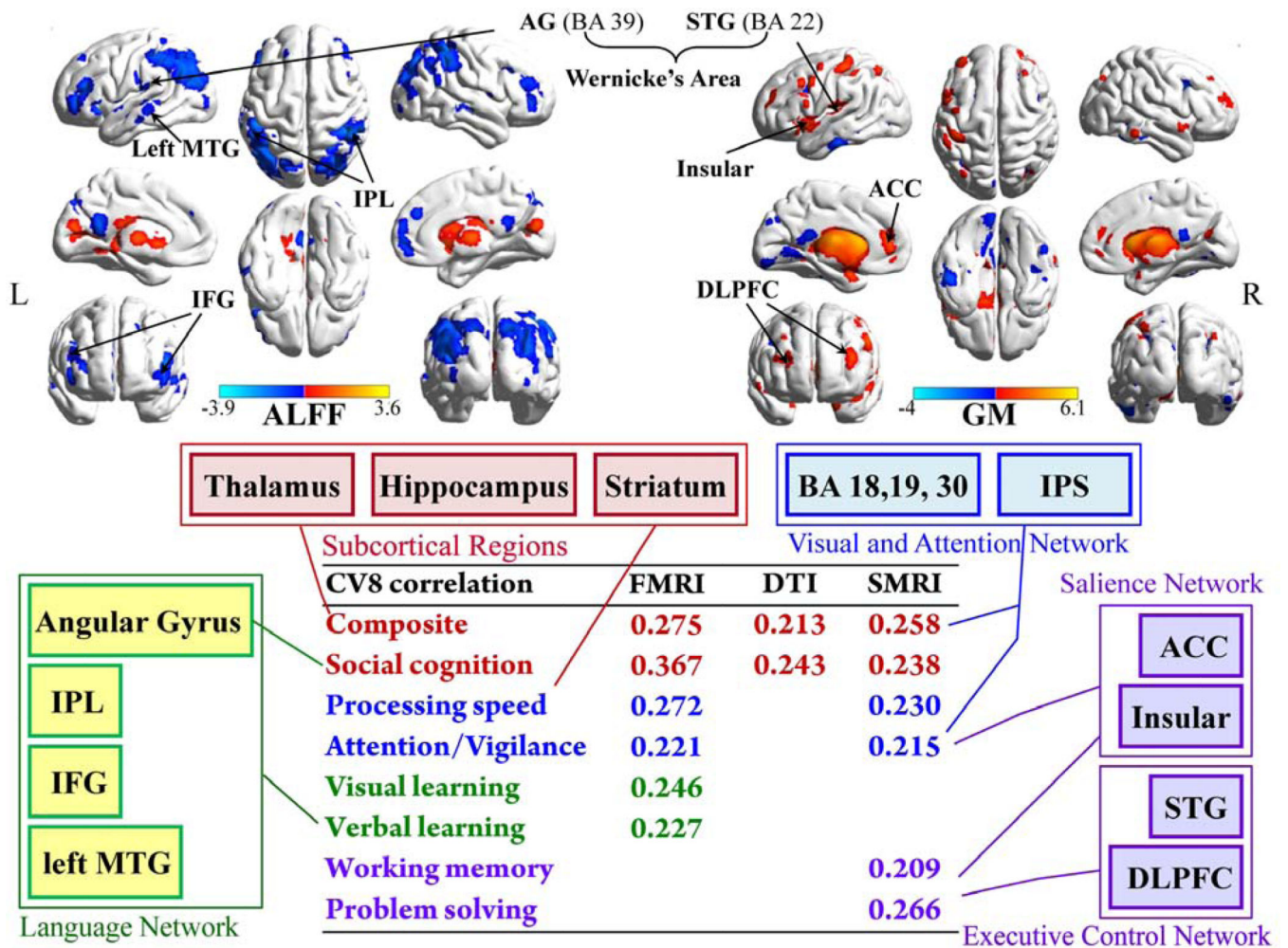


**Figure 4. Cortical maps of fMRI\_CV8 and GM\_CV8, and the summarization of identified brain regions corresponding to the correlated MCCB domains**

Cortical maps of the joint fMRI and sMRI components, and the summarization of identified cortical regions corresponding to their correlated MCCB domains. Note that both subcortical regions (in red frame, some subcortical regions may not show in surface mapping, please see more details in table 2) and visual and attention network (in blue frame) were commonly identified in fALFF and GM, related to composite MCCB and the top 3 domains with which they both correlated. The language network (in green frame) was uniquely detected in fMRI, accompanying the domains of verbal learning, visual learning and social cognition that were particularly correlated with fALFF. Similarly, the salience network and executive control network (in purple frame) that were only discovered in GM could well explain the domains correlate with sMRI only, i.e., working memory and problem solving. Hence the three-way fusion provided a more informative view of co-occurring multimodal abnormalities associated with the specific cognitive deficits in schizophrenia. PHP/HP: parahippocampus/hippocampus.

Table 1

**Demographics and the MCCB scores of the subjects**

Demographic information of the subjects and the correlations between MCCB composite value and specific domains, PANSS symptoms and other measures

Measure	HC	SZ	P*	R*
Number	50	47		
Age	36.7±12.6	35.3±12.6	0.6	0.04
Gender	20F / 30M	6F / 41M	0.01	0.17
Olanzapine equivalent	NA	13.5±9.4		-0.09
Composite	49.8±10.5	31.3±15.7	1.3E-09	1
Speed of processing	51.9±9.0	35.3±13.7	1.5E-09	0.91
Attention/Vigilance	48.3±9.9	36.0±15.1	1.4E-05	0.86
Working memory	46.8±11.4	37.1±14.5	5.3E-04	0.83
Verbal learning	47.4±8.9	38.0±8.6	8.4E-07	0.8
Visual learning	49.3±9.3	36.6±12.6	1.5E-07	0.79
Reasoning/Problem solving	54.2±9.9	46.1±11.7	5.1E-04	0.64
Social cognition	50.8±11.1	40.5±13.0	8.3E-05	0.65
PANSS Negative	NA	15.1±5.4		-0.48
PANSS Positive	NA	15.4±5.9		-0.10

\* MCCB=MATRICES Consensus Cognitive Battery; PANSS= Positive and Negative Syndrome Scale. Olanzapine equivalent= olanzapine total (standardized current dose of antipsychotic medication). P\* denotes the significance value of two sample t-test performed between controls and schizophrenia patients for all measures, except gender (used chi-squared test). R\* is the correlation value between MCCB composite and other measures.

**Table 2**  
**Anatomical information of the identified joint component in CV8**

Anatomic regions of the group-discriminating fMRI component, sMRI component, and the parts of WM tracts identified in dMRI component

<b>fMRI_fALFF</b>			
<b>Area</b>	<b>Brodmann Area</b>	<b>Vol(cc)L/R</b>	<b>Random effects: Max Value (x, y, z)</b>
<b>HC&gt;SZ</b>			
Thalamus		0.3/2.6	2.8 (-3, -14, 3)/3.6 (9, -14, 3)
Caudate/Lentiform Nucleus		2.0/2.7	3.5 (-21, 9, 0)/3.5 (18, 14, -6)
Posterior Cingulate	30	0.6/0.0	3.4 (-21, -64, 6)/NA
Lingual Gyrus/Cuneus	18, 19	1.9/0.2	3.4 (-21, -61, 3)/2.9 (24, -55, 3)
Parahippocampal Gyrus/Hippocampus	19, 30	0.2/0.2	3.1 (-21, -52, 3)/2.7 (21, -52, 3)
<b>SZ&gt;HC</b>			
Middle Temporal Gyrus	19, 21, 39	4.0/0.0	3.9 (-59, -27, -6)/NA
Inferior Parietal Lobule	39, 40	3.3/3.8	3.8 (-48, -33, 46)/3.9 (48, -38, 52)
Angular Gyrus	39	1.3/0.1	3.6 (-45, -62, 36)/2.7 (39, -74, 31)
Precuneus/Superior Parietal Lobule	7, 19, 39	1.1/1.2	3.5 (-39, -71, 34)/3.1 (18, -70, 48)
Superior Occipital Gyrus	19	0.6/0.4	3.4 (-39, -74, 26)/3.2 (33, -80, 29)
Postcentral Gyrus	40	0.2/0.1	3.2 (-50, -33, 49)/2.9 (42, -35, 54)
Inferior/Middle Frontal Gyrus	46	0.9/0.1	2.9 (-45, 36, 12)/NA
<b>sMRI_GM</b>			
<b>Area</b>	<b>Brodmann Area</b>	<b>Vol(cc)L/R</b>	<b>Random effects: Max Value (x, y, z)</b>
<b>HC&gt;SZ</b>			
Caudate		3.0/2.3	6.4 (-9, 12, 10)/5.7 (9, 15, 10)
Thalamus		2.4/2.2	5.4 (-6, -17, 15)/4.8 (3, -14, 12)
Parahippocampal Gyrus	19, 30	1.8/0.6	5.0 (-24, -38, 5)/4.2 (24, -38, 5)
Anterior Cingulate	25	0.5/0.1	4.0 (-3, 11, -3)/3.3 (3, 11, -3)
Lingual Gyrus	18, 19	0.3/0.0	3.6 (-21, -49, 2)/NA
Inferior Frontal Gyrus	47	0.8/0.0	3.4 (-39, 14, -11)/NA
Superior/Transverse Temporal Gyrus	22, 38, 41	1.5/0.0	3.4 (-53, 11, -6)/NA
Middle/Superior Frontal Gyrus	8, 9, 10	1.0/0.2	3.3 (-50, 16, 32)/NA
Superior Parietal Lobule	7	0.1/0.1	2.9 (-33, -67, 50)/2.5 (36, -71, 45)
Postcentral Gyrus	1, 2, 3, 40	0.7/0.0	2.9 (-53, -29, 51)/NA
Insula		0.1/0.0	2.9 (-42, 11, -6)/NA
<b>SZ&gt;HC</b>			
Superior/Middle Frontal Gyrus	6, 8, 9	1.5/2.6	4.1 (-33, 16, 30)/3.7 (36, 13, 30)
Fusiform Gyrus/Middle Temporal Gyrus	20, 37	0.9/0.4	3.4 (-45, -39, -13)/3.3 (45, -33, -16)
Middle Occipital Gyrus	18	0.6/0.5	3.4 (-33, -78, 7)/3.2 (3, -85, -8)
Inferior Parietal Lobule		0.1/0.3	2.5 (-33, -59, 42)/3.1 (50, -42, 24)
Precentral Gyrus	6, 9	0.1/0.3	2.8 (-33, 22, 35)/3.1 (39, 16, 35)
Inferior Temporal Gyrus	20	0.3/0.1	2.9 (-48, -22, -27)/2.8 (53, -30, -16)

Precuneus	39	0.1/0.1	2.7 (-12, -53, 55)/2.8 (36, -62, 34)
Posterior Cingulate	29	0.1/0.1	2.8 (-3, -58, 6)/2.6 (3, -40, 19)
Medial Frontal Gyrus	32	0.0/0.3	NA/2.8 (18, 11, 46)

**dMRI\_FA**

<b>WM tracts</b>	<b>Vol(cc)(L/R)</b>	<b>Percentage</b>	<b>Zmax</b>
<b><i>SZ&gt;HC</i></b>			
Forceps minor/Forceps major	0.1/4.5	0%/9%	2.2(23,45,23)/3.6(17,16,20)
Inferior fronto-occipital fasciculus	2.5/1.6	5%/4%	3.4(16,17,20)/3.2(38,18,22)
Inferior longitudinal fasciculus	1.2/1.9	3%/4%	3(15,18,21)/3.4(38,17,22)
Superior longitudinal fasciculus	0.4/0.8	0%/1%	3.2(30,32,27)/2.8(29,39,26)
<b><i>HC&gt;SZ</i></b>			
Anterior thalamic radiation	1.1/0.3	2%/1%	5.8(23,35,23)/6.9(31,34,24)
Corticospinal tract	2.6/2.2	7%/6%	4.2(24,30,10)/3.1(30,29,10)
Inferior longitudinal fasciculus	0.4/2.3	1%/5%	3.4(11,33,8)/5.4(41,31,10)
Superior longitudinal fasciculus	4.0/3.6	4%/3%	4.2(9,32,9)/5.4(42,32,10)

Table 3

**MCCB and PANSS associations with the joint component**

The MCCB and PANSS associations with joint CV8

Canonical Variant 8	fMRI		dMRI		sMRI	
	<i>r</i>	<i>p</i>	<i>r</i>	<i>p</i>	<i>r</i>	<i>p</i>
<b>Correlation with MCCB</b>						
<i>Composite</i>	0.275	0.007*	0.213	0.046	0.258	0.012
<i>Speed of processing</i>	0.272	0.008			0.230	0.026
<i>Attention/Vigilance</i>	0.221	0.032			0.215	0.037
<i>Working memory</i>					0.209	0.050
<i>Verbal learning</i>	0.227	0.028				
<i>Visual learning</i>	0.246	0.017				
<i>Reasoning/Problem solving</i>					0.266	0.010
<i>Social cognition</i>	0.367	0.0003*	0.243	0.018	0.238	0.021
<b>Corr with PANSS Negative</b>	-0.395	0.006*	-0.286	0.050		
<b>Two sample t-test(p value)</b>		0.006*		0.007*		0.0009*

\* means this correlation passed the FDR correction for multiple comparisons.